Sensitivities of Simulated Convective Storms to Environmental CAPE

CODY KIRKPATRICK*

Earth System Science Center, University of Alabama in Huntsville, Huntsville, Alabama

EUGENE W. MCCAUL JR. AND CHARLES COHEN

Universities Space Research Association, Huntsville, Alabama

(Manuscript received 17 September 2010, in final form 13 April 2011)

ABSTRACT

A set of 225 idealized three-dimensional cloud-resolving simulations is used to explore convective storm behavior in environments with various values of CAPE (450, 800, 2000, and 3200 J kg^{-1}). The simulations show that when CAPE = 2000 J kg^{-1} or greater, numerous combinations of other environmental parameters can support updrafts of at least 10 m s^{-1} throughout an entire 2-h simulation. At CAPE = 450 J kg^{-1}, it is very difficult to obtain strong storms, although one case featuring a supercell is found. For CAPE = 800 J kg^{-1}, mature storm updraft speeds correlate positively with strong low-level lapse rates and reduced precipitable water. In some cases, updrafts at this CAPE value can reach speeds that rival predictions of parcel theory, but such efficient conversion of CAPE to kinetic energy does not extend to all storms at CAPE = 800 J kg^{-1}, nor to any storms in simulations at lower or higher CAPE. In simulations with CAPE = 2000 or 3200 J kg^{-1}, the strongest time-averaged mature updrafts, while supercellular in character, feature generally less than 60% of the speeds expected from parcel theory, and even the strongest updraft found at CAPE = 450 J kg^{-1} fails to reach that relative strength. When CAPE = 2000 J kg^{-1} or more, updrafts benefit from enhanced shear, higher levels of free convection, and reduced precipitable water.

Strong low-level shear and a reduced height of the level of free convection correlate closely with low-level storm vertical vorticity when CAPE is at least 2000 J kg^{-1}, consistent with previous findings. However, at CAPE = 800 J kg^{-1}, low-level vorticity shares the same correlations with the environment as updraft strength. With respect to storm precipitation, in simulations initiated with only 30 mm of precipitable water (PW), all of the storms that last for an entire 2-h simulation tend to produce liquid precipitation at roughly similar rates, regardless of their CAPE. In environments where PW is increased to 60 mm, storms tend to produce the most rainfall at CAPE = 2000 J kg^{-1}, with somewhat lesser rainfall rates at lower and higher CAPE. Nevertheless, over the simulation domain, the ground area that receives at least 10 mm of rainfall tends to increase as CAPE increases, owing to a greater number and size of precipitating updrafts in the domain.

1. Introduction

The pioneering numerical modeling studies of Weisman and Klemp (1982, hereafter WK82) have helped guide convective storm research for nearly three decades. Their work studied storm behavior in an expansive array of convective available potential energy (CAPE) and bulk shear values (Fig. 1), showing dramatic increases in storm updraft velocity as CAPE increased from roughly 1000 to 2000 J kg^{-1}, with persistent updrafts at all values of CAPE above 2000 J kg^{-1} (given sufficient shear). Interestingly, none of the WK82 simulations at CAPE values below about 1000 J kg^{-1} produced a persistent updraft with any appreciable vertical velocity or low-level rotation. However, both observational evidence (e.g., Kennedy et al. 1993; Monteverdi and Quadros 1994; Knupp et al. 1998; Moore et al. 1998; Markowski and Straka 2000; Trapp et al. 2001; Craven and Brooks 2004) and numerical simulations (e.g., McCaul 1991; McCaul and Weisman 1996; McCaul and Cohen 2002; Kirkpatrick et al. 2009) suggest that strong, persistent updrafts can and do exist in such environments. Beyond bulk measures of CAPE or deep-layer shear, additional atmospheric parameters are known to influence the behavior

* Current affiliation: UCAR/COMET Program, Boulder, Colorado.

Corresponding author address: Cody Kirkpatrick, UCAR/COMET, P.O. Box 3000, Boulder, CO 80307.
E-mail: codyk@ucar.edu

DOI: 10.1175/2011MWR3631.1

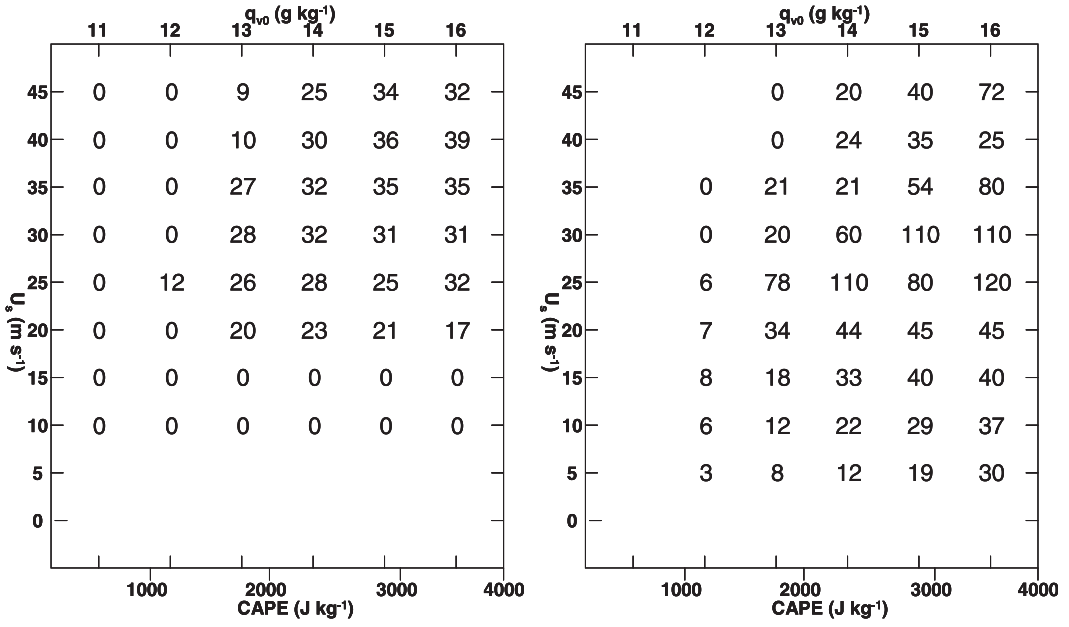

FIG. 1. Adaptations of Figs. 10c and 11 of WK82. (left) Maximum vertical velocity at any model level (m s^{-1}) and (right) vorticity at 178 m (10^{-4} s^{-1}) of simulated storms in the WK82 parameter space study. CAPE is given in units of J kg^{-1} and in terms of boundary layer mixing ratio q_{v0}. Wind shear is given as U_s.

of storm updrafts [e.g., the height of the lifted condensation level (LCL), level of free convection (LFC), and the amount of precipitable water (PW)]. In most observational studies, the relationships between storm properties and these environmental parameters are difficult to quantify since direct measurements of updraft intensity and many other storm properties seldom exist, and the accuracy and representativeness of estimates of even the environmental parameters can be problematic. Instead, updraft strength is usually inferred from overall storm structure, the observable horizontal wind field in conjunction with mass continuity, or the weather produced at the surface (e.g., large hail, tornadoes, etc.).

The theoretical peak vertical velocity of an updraft is related to CAPE by $w_{\max} = (2 \times \text{CAPE})^{0.5}$. This relationship serves only as an estimate, and not an exact forecast of updraft intensity, primarily because of mass loading due to condensate, entrainment of ambient air into the updraft, and the action of pressure perturbation effects. An increase in CAPE (all other environmental parameters held equal) normally leads to an increase in the intensity of simulated updrafts for a variety of storm types, including both squall lines (Takemi 2007) and discrete storms (e.g., James and Markowski 2010; Fig. 8 of Kirkpatrick et al. 2007). Weisman (1993) also found that near-surface wind speeds in simulated storms tended to be stronger as CAPE is increased. However, maximum rainfall rates at the surface do not necessarily exhibit the same linear trends as CAPE increases, either in simulated storms (e.g., Fig. 6 of McCaul et al. 2005) or their observed counterparts (e.g., Marwitz 1972; Fankhauser 1988). It is also not clear how the strength of a storm's low-level rotation is influenced by deep-layer CAPE, although there is evidence suggesting that CAPE in the 0–3-km AGL layer may be related a storm's ability to produce tornadoes (Rasmussen 2003).

The relative influence of other environmental variables on storm behavior can also change as CAPE is raised or lowered. For example, James and Markowski (2010) found that the impact of ambient dry air on simulated updraft intensity is "relatively inconsequential" at CAPE in excess of 4000 J kg^{-1}, but much more important when CAPE was reduced to 1500 J kg^{-1}. The environmental variables explored in this study that are found to exhibit such varied degrees of influence as a function of CAPE will be discussed further in section 3.

It is important to understand storm intensity and morphology under a variety of CAPE conditions because severe weather reports are not confined to any particular range of CAPE values. Although this study is an analysis of *idealized simulated* convective storms, a review of previous climatologies of *observed* storms is appropriate because most of the work associating storm behavior with environmental conditions has been performed using observational datasets. Johns et al. (1993) reported that roughly one-sixth of "significant" tornadoes (F2 or greater) were associated with CAPE values less than 1000 J kg^{-1}. Of proximity soundings associated

with large hail (greater than 5 cm in diameter) and/or tornadoes, Rasmussen and Blanchard (1998, their Fig. 7) found that about half of the soundings had CAPE in a range from 300 to 1900 J kg^{-1}. Numerous other sounding climatologies have also explored the relationships between sounding parameters (including CAPE) and the behavior of deep moist convection (e.g., Rasmussen 2003; Thompson et al. 2003; Craven and Brooks 2004). Consistent with Rasmussen and Blanchard (1998), Craven and Brooks (2004) found a very similar range of CAPE values in their study of proximity soundings associated with hail larger than 5 cm, wind gusts stronger than 33 m s^{-1}, or tornadoes F2 or greater. In soundings analyzed by Thompson et al. (2003), almost three-fourths of the soundings associated with ''supercells'' (Browning 1962, 1964) had CAPE of at least 800 J kg^{-1}. The CAPE calculations in Thompson et al. (2003) and Craven and Brooks (2004) are examples of those that use a mixed-layer parcel, which may obscure reports of hail, wind, or tornadoes associated with ''elevated instability.'' Elevated convection (for which calculations of CAPE using a surface layer or a mixed layer anchored at the surface may be inappropriate), including both discrete storms and quasi-linear convective systems, typically does not produce tornadoes but can frequently produce large hail or strong surface winds (e.g., Colman 1990; Evans and Doswell 2001; van den Broeke et al. 2005; Horgan et al. 2007), implying the presence of strong updrafts and downdrafts.

There is no consensus in the literature about what constitutes ''low'' or ''high'' CAPE. The simulations of Miglietta and Rotunno (2010) include an idealized sounding with only 480 J kg^{-1} of CAPE, and Markowski and Straka (2000) observed a rotating updraft in a ''low-buoyancy'' environment with only about 300 J kg^{-1} of CAPE. A general range of CAPE (less than 1000 J kg^{-1}) was described as low by Geerts et al. (2009), and values of up to 1200 J kg^{-1} have been referred to as ''low to moderate'' (Chin and Wilhelmson 1998). However, ''low'' and ''high'' have also been used to describe much larger values of CAPE (e.g., 1500 and 4500 J kg^{-1}, respectively, in James and Markowski 2010). Furthermore, what is considered low CAPE in the United States might be high in other parts of the world. Brooks et al. (2007) noted that 1000 J kg^{-1} or more of CAPE is not common in the United States (occurring in 7% of 1800 UTC soundings from 1997–99) and is even less so in Europe (approximately 1%). In part because of the rarity of such conditions in Europe, the conditional probability of severe weather there is generally higher given the same values of CAPE and shear (Brooks 2009). Even though a precise definition of low or high CAPE is elusive, and the conditional probability of severe weather (in the United States) is low when CAPE is below roughly 1000 J kg^{-1} (Brooks 2009), such convective environments are ''far more common than environments characterized by high values'' of either CAPE or shear (Dean et al. 2009).

The purpose of this paper is to use results from a set of 225 idealized numerical simulations of isolated convective storms to study storm morphology and intensity as environmental CAPE is changed. The focus is on three important aspects of storm behavior: updraft strength, vorticity production (assumed to be related to the likelihood of tornadoes, in the case of low-level vorticity), and precipitation intensity. The simulations examined are from the Convection Morphology Parameter Space Study (COMPASS; McCaul et al. 2005), a comprehensive set of idealized cloud simulations designed to explore convective storm behavior in a wide range of atmospheric environments. The basic COMPASS simulation set consists of 216 experiments, with 72 conducted at each of three CAPE values (800, 2000, or 3200 J kg^{-1}), and systematic variations in other environmental characteristics imposed at each CAPE; the construction of the various environmental profiles is described in the next section. A series of nine additional simulations was conducted at an even lower CAPE = 450 J kg^{-1}, with the values of other environmental variables chosen based on those which had produced the strongest storms at CAPE = 800 J kg^{-1} (discussed in section 2). The resulting set of 225 COMPASS simulations considered herein offers a diverse array of simulated storms that can be used to examine differences in the sensitivities of storms to their environment at the four different CAPE values. Variations in the other environmental parameters used to design the environmental soundings can also impact storm morphology and intensity, and will be discussed below.

Section 2 contains a summary of the methodology employed in running and analyzing the various COMPASS numerical simulations. Section 3 presents results from the simulation archive, with separate subsections on updraft, storm vorticity, and precipitation characteristics. Section 4 concludes with discussion and summary material, including suggestions for future research efforts.

2. Methodology

Simulations were conducted using an updated edition of the Regional Atmospheric Modeling System (RAMS, version 3b), with improvements described in McCaul and Cohen (2002) and McCaul et al. (2005). The model domain is 75 km on each side, and 24.5 km deep, with a sponge layer in the top 4.5 km. The horizontal grid mesh spacing is 500 m, and the vertical grid spacing is stretched, being 250 m near the ground and 750 m above 20-km altitude. Each experiment is initialized with an

TABLE 1. Parameter choices available for basic COMPASS initial soundings. Here *N* denotes the number of possible values for each parameter, and multiplying all *N*s gives the total number of experiments in the base dataset: 216. Parameter selections for the 9 additional simulations at CAPE = 450 J kg^{-1} are discussed in the text.

Parameter	Acronym	Possible values	*N*
Bulk CAPE	CAPE	800, 2000, and 3200 J kg^{-1}	3
Semicircular hodograph radius	VMAG	8, 12, and 16 m s^{-1}	3
Shape of buoyancy profile	ZMAXB	Two choices per CAPE	2
Shape of shear profile	ZMAXV	Two choices per CAPE	2
LCL–LFC configuration	LCL, LFC	0.5–0.5, 0.5–1.6, and 1.6–1.6 km	3
Cloud-base temperature	T_{LCL}	15.5 or 23.5°C at LCL = 0.5 km	2
RH above LFC	FTRH	Constant, 90%	1

LCL-conserving thermal bubble in an otherwise horizontally homogeneous environment and run for 2 h of simulated time, with saves of all model fields every 5 min. The environmental profiles are constructed using eight variables (Table 1). CAPE (defined from the surface along a pseudoadiabat) takes on one of 3 values, 800, 2000, or 3200 J kg^{-1}, referred to as low, moderate, and high for the purposes of this investigation. An even lower value of 450 J kg^{-1} was added to the experiment design later. The hodographs used are semicircles of varying radius (Fig. 2) through the depth of the domain. The radius of the hodograph is denoted by VMAG, and is allowed to assume a value of 8, 12, or 16 m s^{-1}. Buoyancy and shear profiles are further governed by shape parameters that define the vertical distribution of the quantity in terms of the location of the altitude of maximum buoyancy and v wind (ZMAXB and ZMAXV, respectively). In these simulations, there are two cases for ZMAXB and ZMAXV, referred to as a ''concentrated'' and a ''distributed'' profile case. The distributed profile is one in which the variable (either shear or buoyancy) is spread over a deeper layer with a diffuse maximum in the midtroposphere (high ZMAXV or ZMAXB); in the concentrated profile, the variable maximum is greater in amplitude and peaks in the lower troposphere (low ZMAXV or ZMAXB). The exact altitudes of the maxima are shown in Table 1 of McCaul et al. (2005), and are referred to here as high or low only for simplicity. Concentrated shear profiles have a greater magnitude of low-level shear when compared to the distributed shear profiles (Table 2 of Kirkpatrick et al. 2009). Similarly, the concentrated buoyancy profiles have steeper low-level lapse rates immediately above the LFC relative to distributed buoyancy profiles. Changing ZMAXB has no effect on the lapse rates below the LFC. The range of allowable shape parameters depends on the bulk CAPE.

The LCL and LFC are assigned one of three configurations: 0.5 and 0.5 km, 0.5 and 1.6 km, or 1.6 and 1.6 km. For the cases in which LCL < LFC, the lapse rate in the intermediate layer is moist adiabatic with a 0.5°C dewpoint depression. Cotton and Anthes (1989, 5–6) note that the temperature at the LCL (T_{LCL}) is an effective proxy for atmospheric PW, and our possible values of T_{LCL} are chosen so that PW is roughly 30 mm (T_{LCL} = 15.5°C) or 60 mm (T_{LCL} = 23.5°C). The low-PW case falls within reasonable bounds for environments commonly observed in midlatitude severe storm outbreaks. The high-PW case represents a tropical environment with a warm cloud-base temperature. The terms low and high are relative to one another and are used only for comparison; a PW of 30 mm is not necessarily a low value in the real atmosphere (e.g., Bunkers et al. 2006, their Fig. 9). For each T_{LCL}, the subcloud layers are specified to have constant equivalent potential temperature θ_e, and a lapse rate stable enough to prevent spontaneous mixout of boundary layer moisture and

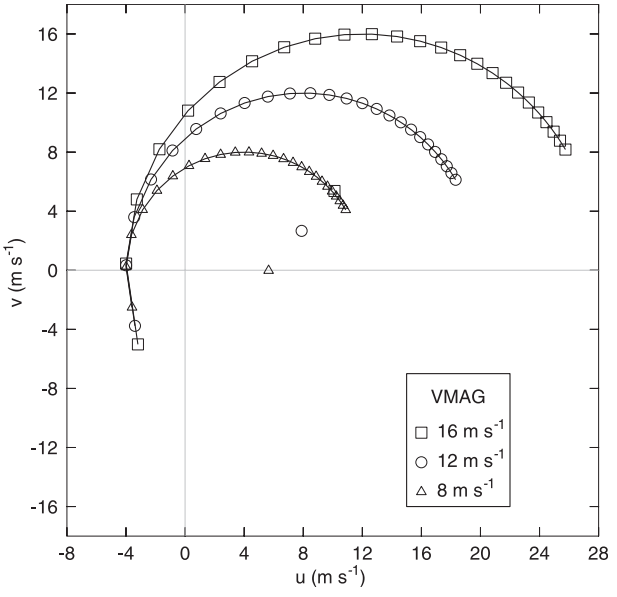

FIG. 2. Sample hodographs (translated) for use in the COMPASS simulations. The hodograph radius (VMAG) is either 8, 12, or 16 m s^{-1}. Each hodograph is translated so that the u wind at 0.5 km is −4 m s^{-1}. Symbols are given every 500 m, from the surface to 12 km AGL. A storm motion estimate using the method of Bunkers et al. (2000) is also shown for each hodograph.

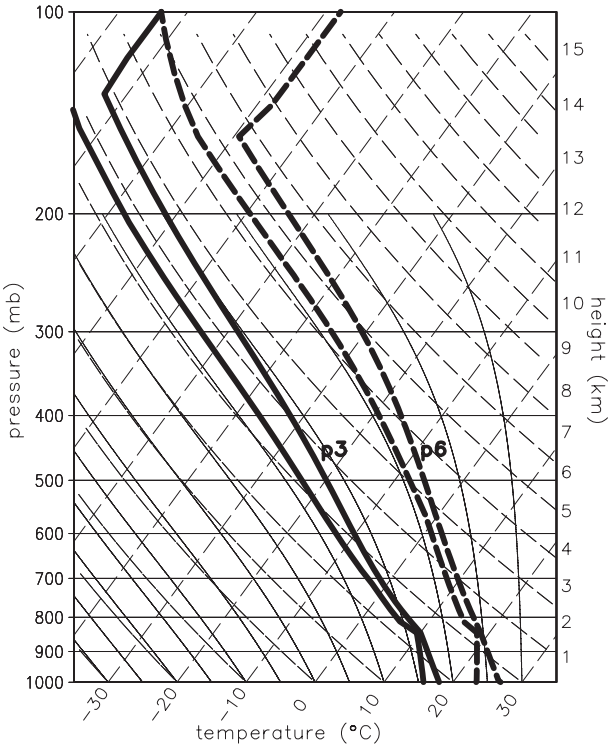

FIG. 3. Example initial thermodynamic profiles for two COMPASS simulations. These two sample profiles have CAPE = 2000 J kg^{-1}, LCL = 1.6 km, and LFC = 1.6 km. The solid lines labeled p3 represent the PW = 30-mm environment, and the dashed lines labeled p6 represent the PW = 60-mm environment.

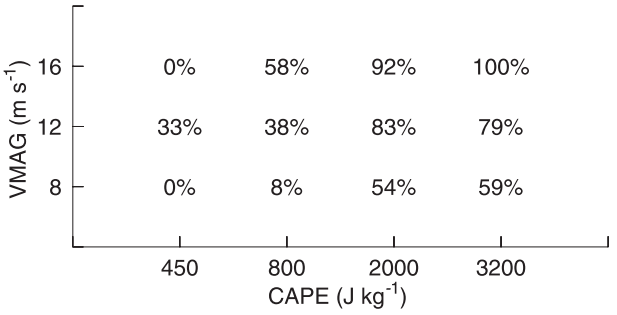

FIG. 4. The percentage of experiments with strong, ''persistent'' storms (as defined in the text) in the COMPASS simulation set, grouped by VMAG (hodograph radius) and CAPE. For CAPE = 450, each entry is comprised of 3 possible experiments; for CAPE ≥ 800, 24 experiments are conducted at each combination of CAPE and VMAG. For example, only 2 of 24 simulations (8%) with VMAG = 8 and CAPE = 800 feature a persistent storm.

shear. In the part of the COMPASS database studied here, an eighth environmental parameter, relative humidity above the LFC [free-tropospheric relative humidity (FTRH)] is fixed at 90%. As a result of all the combinations of the 7 parameters that are allowed to vary here, 216 basic simulations are considered. Two example soundings, illustrating the two possible values of PW but with all other thermodynamic variables held constant, are shown in Fig. 3.

Nine additional simulations were ultimately performed with the lowest CAPE value, 450 J kg^{-1}, mentioned above. In those nine special cases, the three standard values of VMAG were used, along with the three combinations of LCL and LFC described above. Only low ZMAXB and low ZMAXV were used, along with PW = 30 mm, because such conditions were found to promote the strongest storms at CAPE = 800 J kg^{-1}. Although resources did not permit performing a full set of 72 simulations at CAPE = 450 J kg^{-1}, the 9 cases simulated were considered the most likely environments to produce strong convection. These simulations were considerably more sensitive to the choice of initial warm bubble amplitude, with a pronounced tendency to produce transient pulse storms followed by quick cell dissipation. As a consequence, reductions in bubble amplitude to as low as 2.0 K were employed in some cases to promote a more gradual and longer-lasting convective response.

To simplify interpretation of the results, the parameters that determine the particle size distributions of water and ice species are held constant, even though the influence of these parameters has been studied and found to be nontrivial by Cohen and McCaul (2006, 2007) and van den Heever and Cotton (2004). Of the 225 experiments considered here, 140 produce a trackable, right-moving storm with an updraft of at least 2 m s^{-1} that exists throughout a simulation's second hour along with a mean updraft of at least 10 m s^{-1} during that time frame (Fig. 4). We refer to these simulations as producing a ''persistent'' storm for the purposes of this study; these storms are, in reality, both persistent and strong. The threshold values used to define storm persistence and intensity are admittedly arbitrary, and some storms that are strong at the start of the second hour but dissipate or weaken before the end of the simulation have been excluded as a result. Also, some storms that are weakening at the end of a simulation (and would not persist much longer beyond 2 h) may be included. These requirements, in conjunction with the emphasis on the most intense right-moving storms produced in each simulation, combined with the absence of very weak shears and the use of single warm bubble initialization methods in COMPASS, tend to bias the COMPASS results somewhat toward long-lasting unicellular storm morphologies such as supercells. Such bias is not unwarranted, insofar as one of the goals of the COMPASS project is to locate and characterize the boundary between supercell and nonsupercell convective modes in the larger parameter space.

All simulations are originally conducted on a moving domain with the starting hodograph centered at the ground-relative velocity origin. However, to estimate actual ground-relative accumulations of precipitation in these experiments, the simulation results are later translated to emulate storm motions that are more like those commonly observed in the Northern Hemisphere (Fig. 2). The hodographs with the greatest low-level shear bear some resemblance to the hodographs of Esterheld and Giuliano (2008), who found nearly straight-line hodographs in a sample of 18 ''significantly tornadic'' (F2 or greater) proximity soundings, with an embedded kink of nearly 90°. However, the hodographs here feature far more gentle curvature (only 10°–20° difference in angle between model levels, which are spaced at approximately 250-m vertical resolution in the lower troposphere). Sensitivity tests involving the translation of the starting hodographs confirm that storm behavior is Galilean invariant [Klemp and Wilhelmson (1978); Rotunno and Klemp (1982); Rasmussen and Blanchard (1998); see also Bunkers et al. (2000) for a discussion on how storm motion forecasts can be impacted by Galilean invariance]. That is to say, within the eight-dimensional parameter space, grid-relative storm morphology and evolution is the same regardless of the placement of the starting hodograph and the only differences will be in parameters that are calculated in a ground-relative sense.

As in Kirkpatrick et al. (2009), the attributes of the dominant right-moving storm in a simulation are subjected to linear regressions with the environmental parameters of that simulation's starting sounding. In this way, one can correlate particular storm properties with background environmental conditions. Because the seven environmental parameters that comprise each initial profile are largely uncorrelated and can be specified almost completely independently, it is also possible to isolate individual environmental features and their effects on storm morphology. Linear correlations between environmental parameters and certain mature (second hour) storm attributes are explored herein for mean maximum updraft speed at midlevels (WMAX) and at 2 km above the surface (WMAX2), maximum midlevel vorticity (VMAX), maximum vorticity at the lowest model level (126 m AGL; VMAX0), maximum hail mixing ratio aloft (HMAX) and at the lowest model level (HMAX0), maximum rainwater mixing ratio aloft (RMAX) and at the lowest model level (RMAX0), and the total ground area that receives at least 10 mm of liquid precipitation by the end of the simulation (PCPAREA). These storm properties are listed in Table 2 for reference. The linear correlation between RMAX0 and surface precipitation rate is essentially unity ($r^2 = 0.989$), and thus it is safe to use RMAX0 in lieu of surface precipitation rate. Since only two or three values of each environmental parameter are available (Table 1), all regressions are of the linear form. More sophisticated statistical methods, such as principal component analysis, were not used since it was desired to retain as much information about the environmental profile as possible. For all parameters, only two or three choices were used, in order to keep the overall COMPASS project tractable. Although nonlinear storm responses to the environment can be potentially detected for the two parameters that assume more than two possible values (CAPE and VMAG), nonlinear regressions were not pursued because of the small number of variations in the values of each environmental variable. The variance of a storm property's 13 snapshot values averaged from a simulation's second hour (60–120 min, at 5-min intervals) can be used as a measure of temporal variability; these variances are also discussed below. Because the horizontal grid spacing (500 m) is insufficient to resolve tornadoes explicitly, the focus here is on general low-level mesocyclone intensity. This resolution should be sufficient to resolve storm mesocyclones (see Bryan et al. 2003 for a thorough discussion on the influence of grid resolution on simulations of deep moist convection).

TABLE 2. Storm attributes discussed in the text.

Acronym	Attribute
HMAX	Maximum hail mixing ratio aloft
HMAX0	Maximum hail mixing ratio at 126 m
PCPAREA	Total ground area that received at least 10 mm of precipitation
RMAX	Maximum rainwater mixing ratio aloft
RMAX0	Maximum rainwater mixing ratio at 126 m
TMASS	Total mass of rainwater produced
VMAX	Maximum vertical vorticity aloft
VMAX0	Maximum vertical vorticity at 126 m
WMAX	Maximum updraft velocity aloft
WMAX2	Maximum updraft velocity at 2 km

The Pearson product moment correlation coefficient r is calculated for many of the storm–environment relationships discussed herein (e.g., Table 3). For a bivariate dataset with N pairs of data, the statistical significance of a correlation coefficient (i.e., H_0: $r = 0$; H_1: $r \neq 0$) can be evaluated by computing the test statistic $t = r\sqrt{(N-2)/(1-r^2)}$, which has Student's distribution with $N - 2$ degrees of freedom [e.g., Eq. (11.46) of Montgomery and Runger 2003]. In this paper, the alternate hypothesis (H_1) is accepted if t falls within the top or bottom 2.5% ($\alpha = 0.05$) of the distribution. As an example, $N = 72$ for each r reported in Table 3, and thus $|r|$ must be greater than 0.23 for $|t|$ to exceed the critical value of 1.99.

TABLE 3. Linear correlation coefficients between environmental parameters and second-hour average updraft velocity (WMAX), as a function of CAPE. The number of simulations conducted at each CAPE value is shown as *N*. Correlations with magnitude above the critical value at $\alpha = 0.05$ (0.23 for $N = 72$; 0.67 for $N = 9$) are shown in bold. For the CAPE = 450 storms, all 9 simulations had the same values of ZMAXB and ZMAXV.

	CAPE (J kg^{-1})			
	450	800	2000	3200
VMAG	0.06	**0.27**	**0.55**	**0.60**
ZMAXB	N/A	**−0.65**	−0.20	−0.19
ZMAXV	N/A	−0.14	**−0.26**	**−0.24**
LCL	0.65	0.09	0.17	0.09
LFC	0.45	**0.27**	**0.50**	**0.43**
T_{LCL}	−0.65	**−0.33**	**−0.48**	**−0.44**
N	9	72	72	72

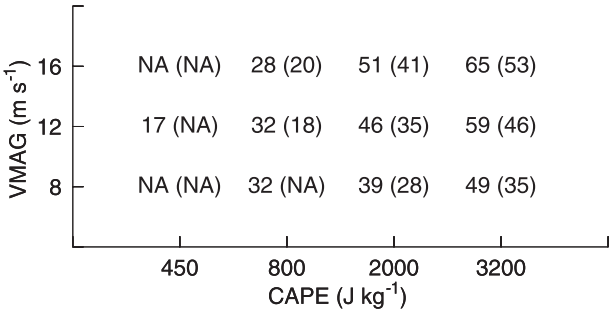

FIG. 5. The peak second-hour WMAX (m s^{-1}) for persistent right-moving storms. Binned by CAPE and VMAG as in Fig. 4, with further stratification also given by environmental PW. Each table entry is the average of all experiments that produce persistent storms with those CAPE, VMAG, and PW values. The average value for all storms with low PW (30 mm) is given at left, and for high PW (60 mm) in parentheses. Only the 140 persistent storms (whose distribution is shown in Fig. 4) are included. The NA means no persistent storms occurred in any of the simulations with those values of CAPE, VMAG, and PW. No simulations were conducted at CAPE = 450 and PW = 60.

3. Results

For each combination of CAPE and VMAG in the basic COMPASS parameter space (Table 1), the number of experiments that produce strong, persistent storms increases as either CAPE or VMAG increases (Fig. 4). In fact, all 24 experiments at the combination of the largest CAPE and VMAG values feature persistent convection. For reasons described below, storms persist for the entire 2-h simulation in relatively few (25 of 72, or 35%) of the CAPE = 800 environments, and only 1 of the 9 simulations at CAPE = 450. Increasing VMAG produces a much greater relative increase in the number of persistent storms at CAPE = 800 than it does at either of the higher CAPE values (Fig. 4). Interestingly, mean peak updraft velocity (WMAX) is very nearly the same in all VMAG groups when CAPE is fixed at 800 J kg^{-1} (Fig. 5). When CAPE = 2000 or 3200, WMAX increases as CAPE increases or as VMAG increases, for both values of PW. Unlike WK82 (reproduced in Fig. 1 herein), simulations with the largest VMAG value do not produce storms with weaker WMAX, although the total shears in the present experiments with the largest VMAG are comparable to those in WK82. We suspect that the decrease would begin to appear if simulations were performed with VMAG greater than 16 m s^{-1}, further increasing the shear over the depth of the troposphere.

Examples of storm structure at selected times for a subset of VMAG = 12 and VMAG = 16 simulations at CAPE = 450 are shown in Figs. 6 and 7. Each snapshot is selected from late in the simulation's second hour, to provide a rough overview of mature storm appearance. In each figure, all environmental parameters are held constant except for CAPE. These figures illustrate the general progression in storm structure that is seen as CAPE is increased. Because of the tendency for LCL = LFC = 1.6 km to produce the strongest updrafts at all values of CAPE studied (Table 3), that LCL–LFC configuration is shown in Figs. 6 and 7. For VMAG = 12 m s^{-1} (Fig. 6), all of the storms with CAPE ≥ 800 J kg^{-1} contain updrafts stronger than 20 m s^{-1} at 3.5 km AGL (shown in the figure), and between 30 and 70 m s^{-1} higher aloft (increasing as CAPE increases). However, as shown in Table 4, no updraft in the CAPE = 450 simulations ever reaches an intensity above 17 m s^{-1} at any time in the second hour, at any vertical level. The CAPE = 450 simulations also never produce a storm with a "left split" (not shown), in contrast to simulations with greater values of CAPE. Finally, in Fig. 7 observe that all of the storms with CAPE of at least 800 J kg^{-1} have a somewhat similar qualitative appearance, with a strong updraft core and a larger precipitation footprint than the storm in the CAPE = 450 simulation. Based on this limited sample, it appears that substantial changes in simulated storm characteristics can occur as CAPE is reduced from 800 to 450 J kg^{-1}, although storms with supercell characteristics are still possible at that lowest CAPE value.

a. Implications for updraft intensity

In Kirkpatrick et al. (2009), CAPE, VMAG, and T_{LCL} were the three parameters that collectively explained most of the inter-experiment variance in WMAX (61%, out of a total 81% when all 7 parameters are used; their Table 3). However, when only the CAPE = 800 simulations are considered, the vertical level of maximum buoyancy (ZMAXB) becomes the most important parameter (Table 3). This finding was obscured in the analysis conducted by Kirkpatrick et al. (2009), where the entire simulation dataset was studied as a single group,

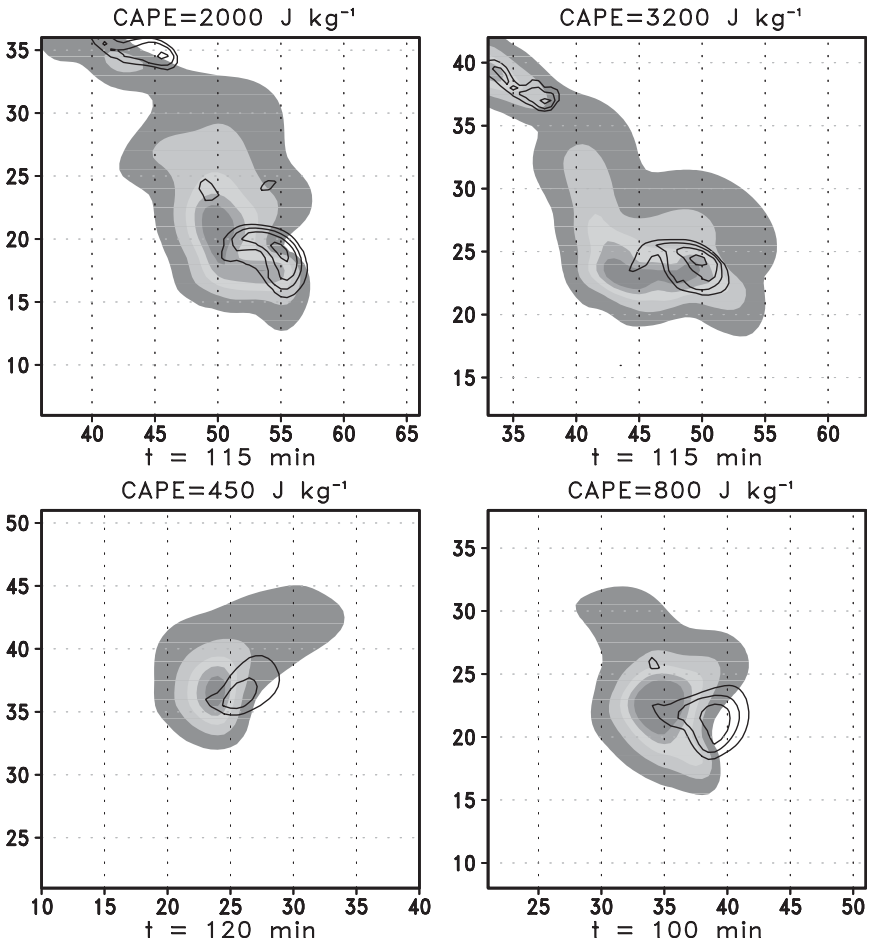

FIG. 6. Maps of simulated updraft velocity at 3.5 km for CAPE values of 450, 800, 2000, and 3200 J kg^{-1} (contoured at 5, 10, 15, 20, 25, and 30 m s^{-1}) and rainwater mixing ratio at 126 m (shaded at 0.25, 1, 2, 3, and 4 g kg^{-1}) for simulations with constant VMAG (12 m s^{-1}), low ZMAXB and ZMAXV, LCL = LFC = 1.6 km, and PW = 30 mm. Axes are in km. Each plot is taken from the last 20 min of its simulation, at a time deemed representative of mature storm structure.

without examining subsets based on the CAPE value of the starting sounding in each experiment. Decreasing the height of ZMAXB, that is, increasing the lapse rates just above the LFC, enhances WMAX at all values of CAPE (Fig. 8), but especially so at CAPE = 800. All of the 25 simulations with persistent storms at CAPE = 800 feature low ZMAXB and thus more buoyancy in the layer just above the LFC. Essentially, when CAPE = 2000 or 3200, lowering ZMAXB produces a 20%–30% increase in WMAX, but at CAPE = 800, lowering ZMAXB (which is analogous to steepening the low-level lapse rates) *increases WMAX by as much as 500% and can mean the difference between persistent convection and storm demise* (Fig. 8). These results are consistent with McCaul and Weisman (2001), but show how the effects play out in the greater thermo-kinematic parameter space.

As an example, consider time–height cross sections of updraft velocity for the two storms shown in Fig. 9. The environments of the two storms have *only* the level of maximum buoyancy (ZMAXB) changed. In the distributed buoyancy simulation (top panel), the updraft forced by the initiating thermal impulse is strong (greater than 20 m s^{-1}), but weakens quickly. There is a period of over 20 min when the updraft is not stronger than 10 m s^{-1} at any level (although it remains trackable). Eventually, the updraft does restrengthen slightly, and for this simulation (the second-hour mean) WMAX is about 14 m s^{-1}. This storm is the strongest persistent storm in the 36 simulations with high ZMAXB and CAPE = 800. When the buoyancy profile is changed to the low-ZMAXB case (bottom panel), after initiation the updraft remains stronger than 20 m s^{-1} throughout the rest of the simulation, with pulses of greater than 30 m s^{-1} occurring

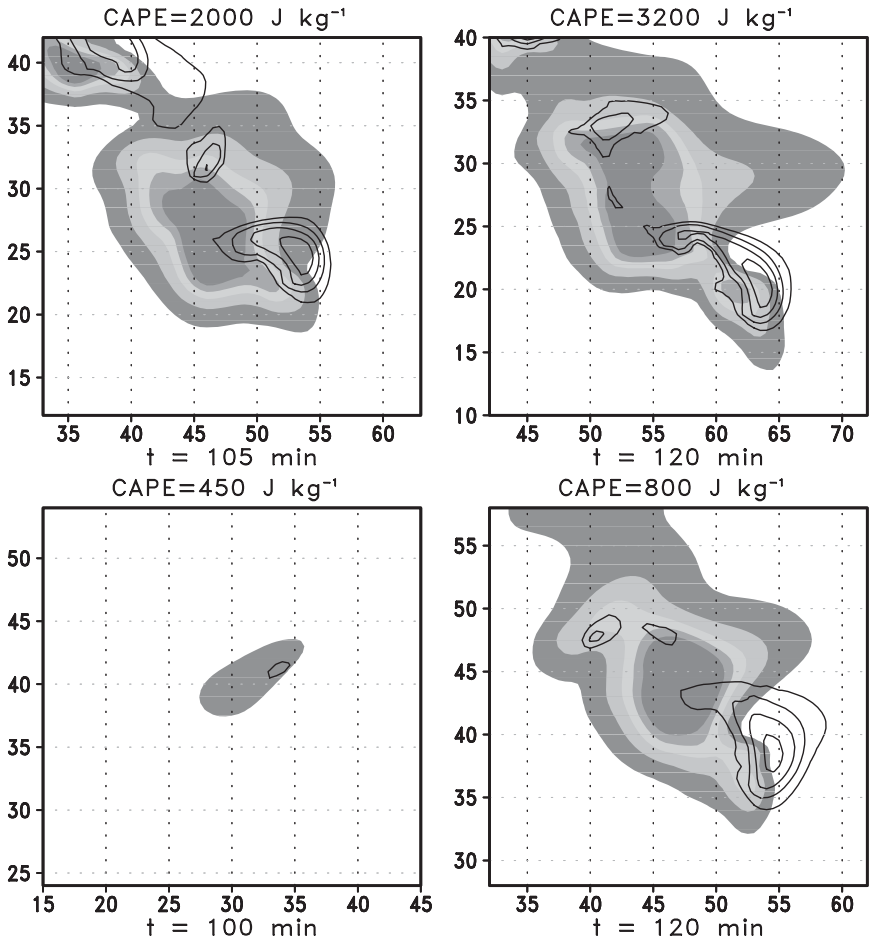

FIG. 7. As in Fig. 6, but for VMAG = 16 m s^{-1}.

at least 3 times during the full 2-h experiment. The storm in the concentrated buoyancy environment features a mean second-hour WMAX of 29 m s^{-1}, a more than 100% increase over its distributed buoyancy counterpart, and an extreme instantaneous updraft speed of 35 m s^{-1}, 88% of the peak value expected from parcel theory. For other storms in the CAPE = 800 regime, the shift from high ZMAXB to low ZMAXB induces even larger relative increases in WMAX, sometimes nearing 500%. Three of the 72 simulations conducted at CAPE = 800 produce updrafts with peak instantaneous speeds *in excess* of the expected parcel theory value of 40 m s^{-1}; all three feature our low value of ZMAXB, ZMAXV, and PW, and the high value of LFC.

Although VMAG (i.e., hodograph radius) is the dominant predictor of WMAX at CAPE = 2000 and 3200, updraft speeds at CAPE = 800 are essentially unchanged as VMAG is varied (differing by an average of 4 m s^{-1}; Fig. 5). Instead, at CAPE = 800, as VMAG is increased there is a pronounced increase in the number of simulations that produce strong, persistent storms (Fig. 4). For example, none of the 12 experiments with CAPE = 800 and 30 mm of PW produce a persistent storm when VMAG = 8, but 4 of 12 do for VMAG = 12, and 6 of 12 for VMAG = 16. Updrafts (including those at CAPE = 800) in the simulations initialized with 60 mm

TABLE 4. Maximum vertical velocity ("Max *W*") attained in a simulation's second hour for the 9 special simulations with CAPE = 450 J kg^{-1}, low ZMAXB, low ZMAXV, and low PW. The simulation time at which the maximum velocity is reached is also shown.

VMAG (m s^{-1})	LCL (km)	LFC (km)	Max *W* (m s^{-1})	Time (min)
8	0.5	0.5	7.2	60
8	0.5	1.6	10.5	60
8	1.6	1.6	9.6	60
12	0.5	0.5	6.0	60
12	0.5	1.6	7.0	85
12	1.6	1.6	16.5	120
16	0.5	0.5	4.4	60
16	0.5	1.6	3.0	85
16	1.6	1.6	6.9	95

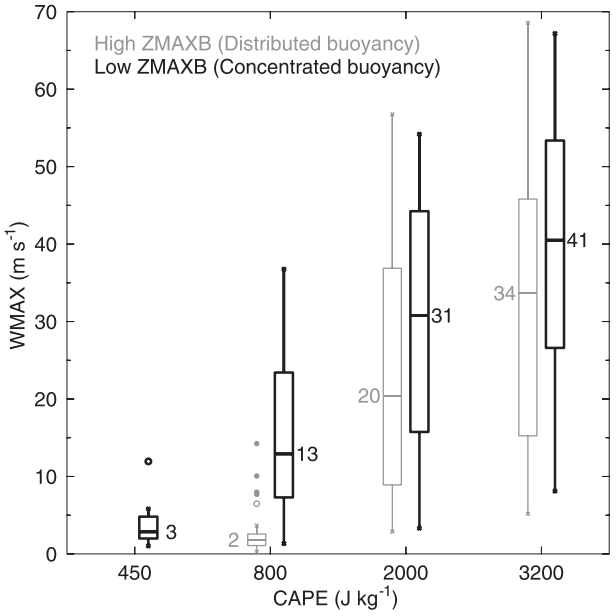

FIG. 8. Box plots illustrating the influence of changing the vertical distribution of buoyancy on second-hour WMAX. Simulations with low ZMAXB are shown in black, high ZMAXB in light gray. All 225 experiments are shown. Each box plot shown consists of 36 unique experiments for CAPE ≥ 800, and 9 experiments for CAPE = 450. No simulations were conducted at CAPE = 450 and high ZMAXB. The box edges show the first (q1) and third (q3) quartiles, and the whiskers extend to the farthest data points that are still within a distance of 1.5 interquartile ranges from q1 and q3. Outliers beyond the whiskers are shown, in open circles up to a distance of three interquartile ranges beyond q1 or q3, and in closed circles beyond that. The median WMAX for each distribution is also shown.

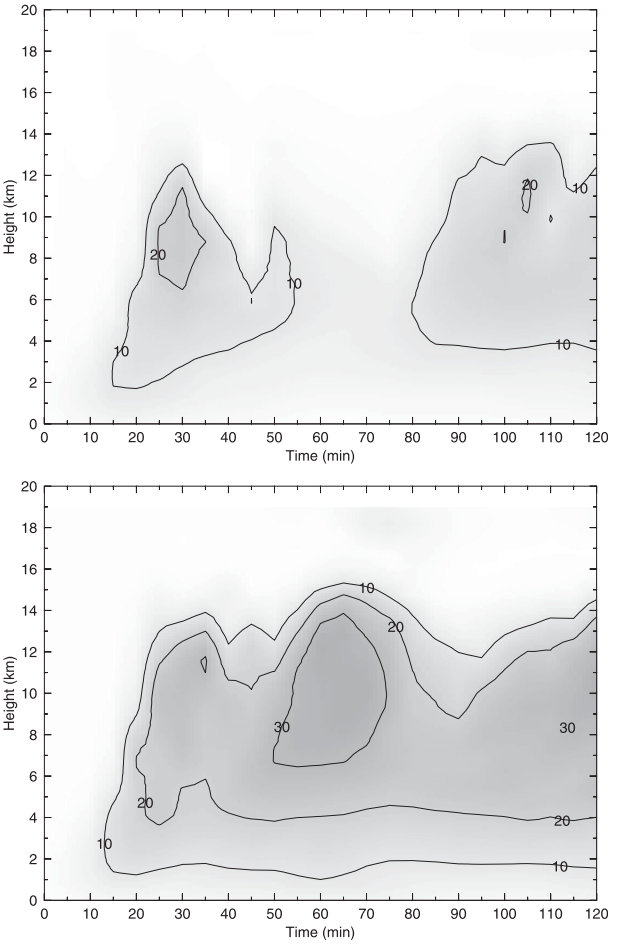

FIG. 9. Time–height series of updraft velocity (WMAX; m s^{-1}) for the dominant right-moving storm in the domain of two simulations with only ZMAXB varied. (top) The high-ZMAXB case and (bottom) the low ZMAXB case. Both simulations have CAPE = 800 J kg^{-1}, VMAG = 16 m s^{-1}, the high value of ZMAXV, LCL = 0.5 km, LFC = 1.6 km, and PW = 30 mm.

of PW produce more condensate than those in the 30-mm PW simulations, and in the absence of sufficient vertical wind shear (e.g., at VMAG = 8), most of this condensate falls back into the updraft. A qualitative examination of the CAPE = 800, VMAG = 8, and PW = 60 simulated storms reveals that they tend to resemble short-lived, single-cell ''pulse'' convection. Consider also that for the 140 simulations with persistent storms, average updraft strength at 2 km AGL (WMAX2) is similar for the 56 high-PW (8.5 m s^{-1}) and 84 low-PW (9.8 m s^{-1}) storms, but *peak* strength in the updrafts aloft is markedly different (29 vs 39 m s^{-1}).

Table 3 shows that when all 72 of the CAPE = 800 simulations are considered, there exists a positive correlation (0.27) between WMAX and VMAG. Much of this positive correlation comes from a small number of cases in the VMAG = 12 or VMAG = 16 environments where peak WMAX approaches 40 m s^{-1}, the value predicted by parcel theory. This correlation may also be biased because it includes the 47 simulations at CAPE = 800 that do not produce persistent storms. Increasing VMAG at CAPE = 800 moves the bulk Richardson number (BRN) from about 30 (at VMAG = 8) to about 10 (at VMAG = 16), near the range of BRN values where environments become excessively sheared and updraft speed and duration might be expected to decrease. In fact, with some exceptions, in the 25 persistent CAPE = 800 storms there is a tendency for a slight *decrease* in average WMAX as VMAG increases (Fig. 5; $r = -0.20$ for these experiments). This correlation, however, is not statistically significant at even the $\alpha = 0.10$ significance level.

As discussed in McCaul and Cohen (2002, their Fig. 12a) and Kirkpatrick et al. (2009, their Fig. 1a), raising the LFC (within the range of 0.5–1.6 km) tends to increase WMAX, and this trend is seen at all 4 values of CAPE studied here (Table 3). The correlation between LFC and WMAX is statistically significant for experiments with CAPE ≥ 800 J kg^{-1}. McCaul and Cohen (2002)

showed how a higher LFC reduces entrainment of ambient low-θ_e air that usually resides above the LFC, generally resulting in less updraft dilution and greater updraft area. However, although a raised LFC usually enhances WMAX, it is often detrimental to low-level rotation, as will be described in the next section.

In contrast to LFC, LCL height has no statistically significant linear correlation to WMAX for any value of environmental CAPE (Table 3). Examination of the correlations between LCL height and numerous other storm properties (midlevel updraft area and midlevel vorticity, discussed below, and storm motion, discussed in Kirkpatrick et al. 2007) also failed to yield any statistically significant links. LCL height, on the other hand, does correlate negatively to the occurrence of *supercells* in the simulations (not shown), defined by their second-hour average midlevel vorticity (VMAX, greater than 0.01 s^{-1}) and vertical velocity–vertical-vorticity correlation coefficient (0.4 or greater; WK82). In simulations where the LCL is held at 0.5 km, 56% (51 of 91) of the persistent storms are supercells. Only 44% (21 of 48) of persistent storms are supercells in simulations with the LCL at 1.6 km. The velocity–vorticity correlation coefficient tends to be higher for storms in the LCL = 0.5-km simulations (0.63 vs 0.53 for LCL = 1.6 km), and Droegemeier et al. (1993) have discussed how this coefficient may be used to predict storm type.

The results of all 9 simulations at CAPE = 450 are summarized in Table 4. The simulations with VMAG = 8 and VMAG = 16 both produce updrafts generally weaker than those at VMAG = 12; the VMAG = 8 storms were the weakest, and at VMAG = 16 the strongest storm occurred at LCL = LFC = 1.6 km, reaching a peak WMAX of only 7 m s^{-1} in the second hour. For CAPE = 450 and VMAG = 16, the BRN is less than 4; it is highly likely that these storms are unable to persist owing to the extreme imbalance between CAPE and shear.

Only 1 of the 9 simulations at CAPE = 450 produced a persistent updraft. The simulation with VMAG = 12 and LCL = LFC = 1.6 km produces the strongest storm, with a trackable updraft having a second-hour mean WMAX of 11.9 m s^{-1} (a snapshot of this storm is shown in Fig. 6). The extreme peak updraft of the storm is 17 m s^{-1} (Table 4), but this value is still less than 60% of the 30 m s^{-1} that parcel theory predicts might be possible. As for the VMAG = 8 and 16 cases, the LCL = LFC = 0.5-km simulations produce transient storms that weaken sharply after the initial thermal impulse and cannot be tracked for the full 2 h.

b. Implications for storm vorticity

In typical U.S. Great Plains severe storms environments, large amounts of CAPE and shear are generally favored for strong, rotating storms (Maddox 1976; Kerr and Darkow 1996; Rasmussen and Blanchard 1998; Rasmussen and Straka 1998; Thompson and Edwards 2000; Markowski et al. 2003; Thompson et al. 2003). Table 5 suggests that VMAG is the dominant environmental parameter when explaining maximum midlevel vertical vorticity (VMAX) in simulations with at least 2000 J kg^{-1} of CAPE.[1] No other environmental variable has any significant correlation with VMAX when CAPE = 2000 or 3200. For vorticity *near the surface* (VMAX0), however, when CAPE is at least 2000 J kg^{-1} numerous environmental parameters become important to varying degrees, as indicated by the correlations listed in the table. This is not surprising, as each of these parameters has been identified independently in the literature as being important for low-level rotation in observed storms. Specifically, Table 5 shows that, at CAPE = 2000 or 3200, VMAX0 tends to increase when: deep-layer and low-level shear are increased (increasing VMAG and lowering ZMAXV; e.g., Markowski et al. 2003); the LCL is lowered from 1.6 to 0.5 km (e.g., Rasmussen and Blanchard 1998); lapse rates above the LFC are increased (lowering ZMAXB, also analogous to increasing 0–3 km CAPE,[2] as described in Rasmussen 2003); and, especially,

TABLE 5. Linear correlation coefficients between environmental parameters and midlevel (VMAX) and near-surface (VMAX0) vertical vorticity. Persistent storms at CAPE = 800 are shown on the left, and persistent storms at either CAPE = 2000 or 3200 are shown on the right. Correlations with an absolute value that is statistically significant at $\alpha = 0.05$ are shown in bold (for CAPE = 800, $N = 25$ and the critical r is 0.38; for the group that includes both CAPE = 2000 and 3200, $N = 114$, and the critical r is 0.19). No correlation coefficient can be calculated for VMAX or VMAX0 vs CAPE in the CAPE = 800 cases, since only one CAPE value is considered. The last line shows the amount of variance explained by the environmental profile when using a seven-parameter, multiple linear regression.

	CAPE = 800		CAPE = 2000 or 3200	
	VMAX	VMAX0	VMAX	VMAX0
CAPE	n/a	n/a	**0.27**	0.01
VMAG	−0.01	0.12	**0.68**	**0.63**
ZMAXB	**−0.46**	−0.33	−0.01	**−0.27**
ZMAXV	**−0.50**	**−0.42**	−0.13	**−0.25**
LCL	0.18	−0.05	0.04	**−0.25**
LFC	0.20	−0.18	0.14	**−0.35**
T_{LCL}	**−0.40**	**−0.40**	−0.05	0.07
Multiple r^2	0.68	0.79	0.83	0.78

[1] In Table 5, the CAPE = 450 group is excluded. Only one persistent storm occurred in the nine simulations conducted at that CAPE value; as a result, no correlations can be calculated for VMAX or VMAX0.

[2] Shifting ZMAXB from the high to the low value increases 0–3 km CAPE from roughly 30 to 100 J kg^{-1}.

lowering the LFC from 1.6 to 0.5 km (e.g., Davies 2004). The positive correlation between CAPE and VMAX ($r = 0.27$) in these simulations, but lack of correlation between CAPE and VMAX0 ($r = 0.01$), is consistent with CAPE's known inability to serve as a supercell versus tornado discriminator in the observational record (e.g., Rasmussen and Blanchard 1998). No statistically significant correlation between VMAX or VMAX0 and T_{LCL} is seen when CAPE is either 2000 or 3200 J kg^{-1} (Table 5); essentially, strong rotation—both aloft and at low levels—is possible regardless of environmental temperature of atmospheric PW, if CAPE is large enough.

However, when studying VMAX and VMAX0 in storms at CAPE = 800, a different and distinctive pattern of important environmental parameters emerges. First, the behaviors of VMAX and VMAX0 are more similar to one another at CAPE = 800 than for the moderate- and high-CAPE categories (Table 5), in part because the simulated updrafts at this CAPE value tend to be somewhat less deep. For example, the mean altitude of WMAX for the CAPE = 800 storms is only 6.4 km, but is 9.6 and 10.5 km for the CAPE = 2000 and CAPE = 3200 groups, respectively (see also McCaul and Weisman 1996). The three parameters that relate most closely (in a linear correlation sense) to VMAX0 at CAPE = 800 are the same as those for VMAX: T_{LCL}, ZMAXB, and ZMAXV (Table 5). Thus, in simulations where CAPE = 800, VMAX and VMAX0 are larger in the simulations with our low value of T_{LCL}, and the low choice of vertical levels of maximum buoyancy (ZMAXB) and shear (ZMAXV). At this CAPE value, these three parameters combined account for 45% of the variability in VMAX0 and 61% for VMAX. McCaul and Weisman (2001) have demonstrated the enhancements to VMAX and VMAX0 that can occur for low values of ZMAXB and ZMAXV, specifically when CAPE = 800. Increasing the magnitude of low-level shear (by decreasing the level of maximum v wind, ZMAXV, in the COMPASS semicircular hodographs) provides more environmental surface relative humidity (SRH) for tilting by the updraft, and simulations with a low ZMAXV have increased 0–1 km and 0–3 km SRH compared to their high-ZMAXV counterparts.[3] The trend is especially noticeable at CAPE = 800. For the CAPE = 800, VMAG = 16 simulations, those with high ZMAXV have an average SRH of 35 m^2 s^{-2}, and the simulations with low ZMAXV have an average of SRH of 131 m^2 s^{-2}, over 3 times the value of the high-ZMAXV cases. This compares with simulations at the CAPE values of 2000 J kg^{-1} or more (and with VMAG = 16), where the SRH in high-ZMAXV simulations is similar (31 m^2 s^{-2}), but does not increase as much for those with low ZMAXV (78 m^2 s^{-2}), all other environmental parameters held constant. At CAPE = 800, shifting to the low-ZMAXV profile increases SRH (in the 0–1-, 0–3-, and 0–6-km layers), and also leads to 3–5 m s^{-1} increases in WMAX at 2 km AGL (not shown), and a doubling or tripling of VMAX0 in most cases. Although Adlerman and Droegemeier (2005) considered only one thermodynamic profile in their study of mesocyclone behavior as a function of the shear profile, in our dataset we also find that "in general, the strongest mesocyclone rotational intensity occurs when the largest shears are confined to the shallowest depths" (Adlerman and Droegemeier 2005, p. 3619).

Reduced LCL height also bears a statistically significant correlation with VMAX0 when CAPE = 2000 or 3200 (Table 5), similar to the relationships that have been found in observational studies of LCL heights and tornadoes (Rasmussen and Blanchard 1998; Thompson et al. 2003; Craven and Brooks 2004). In an observational study that specifically addresses only convection with CAPE below roughly 1000 J kg^{-1}, Davies (2006b) found that LCL heights were generally lower as the strength of reported tornadoes increased, although this relationship was much less obvious when the analysis was confined to certain environmental regimes, such as tornadoes associated with tropical cyclones (Davies 2006a). The correlations in Table 5 show that, at CAPE = 800, in the present simulation database there is no statistically significant relationship between LCL height and VMAX0.

Correlations of LFC to near-surface storm vorticity also behave in a complex way. In both the low (800 J kg^{-1}) and moderate to high (2000–3200 J kg^{-1}) CAPE bins, LFC height demonstrates positive correlations with VMAX, but *negative* correlations to VMAX0 (Table 5). When CAPE = 2000 or 3200, the strongest VMAX occurs when LFC heights are at our high value (1.6 km), but the strongest VMAX0 occurs when the LFC is at the low value (0.5 km). The trends are similar though not as pronounced at CAPE = 800. We believe the apparent contradictions in the sensitivities of VMAX and VMAX0 to LFC height can be resolved as follows. McCaul and Cohen (2002) showed that as the LFC is raised (steadily from 0.5 to 1.6 km in their simulations), updraft overturning efficiency, strength, and rotation at midlevels steadily increase, associated with reduced entrainment and systematic increases in both updraft diameter and mean equivalent potential temperature in the updraft core. However, as the LFC is lowered (again, from 1.6 to 0.5 km), more CAPE is available to the low-level updraft, which promotes stronger updraft accelerations and thus

[3] SRH is calculated using the *simulated* storm motion (averaged over each simulation's second hour, as in Kirkpatrick et al. 2007), not an estimate of storm motion (e.g., the method described by Bunkers et al. 2000).

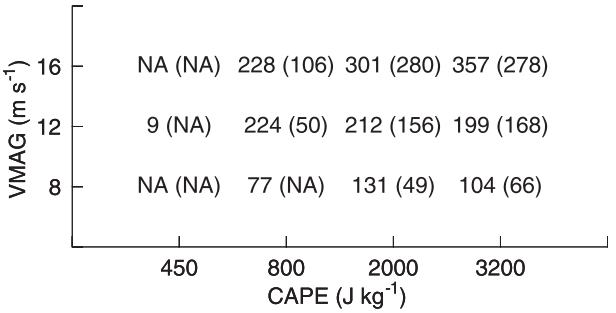

FIG. 10. As in Fig. 5, but for peak second-hour VMAX0 (10^4 s^{-1}).

enhanced stretching of vorticity at low levels. In observed storms, Rasmussen (2003, p. 532) has also hypothesized that increasing the amount of low-level CAPE may promote "more effective interaction between low-level shear and the low-level updraft, thereby augmenting ascent and strength through the nonhydrostatic pressure field" (see also Rotunno and Klemp 1982). The relationship between LFC height and VMAX0 (and VMAX) is less obvious in the simulations where CAPE = 800 J kg^{-1}, because of the smaller sample size and the dominance of the effects of ZMAXB, ZMAXV, and T_{LCL} at that CAPE value (Table 5).

When the 140 persistent storms are binned by CAPE and VMAG (and PW; Fig. 10), only at the largest hodograph radius (VMAG = 16 m s^{-1}) does increasing CAPE produce a clear increase in VMAX0 (neglecting the one persistent storm at CAPE = 450). At VMAG = 12 and VMAG = 8, BRN values exceed 100 for CAPE = 3200, which is beyond the range expected to produce convection with sustained low-level rotation (this is true even though those updrafts may temporarily be strong at upper levels; Fig. 5). However, when CAPE is fixed at either 2000 or 3200 J kg^{-1}, 50%–100% increases in VMAX0 occur as the hodograph radius is increased, demonstrating the strong correlations between VMAG and VMAX0 seen at those CAPE values in Table 5. As discussed with WMAX above, in the WK82 simulations (Fig. 1) VMAX0 declines as bulk shear is increased beyond some ideal value; this peak followed by a decline is not present in the COMPASS simulation database (Fig. 10).

Midlevel vorticity (not shown) for the lone persistent storm at CAPE = 450 achieves VMAX values comparable to those seen in the supercells at CAPE = 800, but near-surface vorticity VMAX0 is only about 5%–10% of the values seen there (Fig. 10; also, the surface rainfall footprint and updraft at 3.5 km for this storm are shown in Fig. 6). However, this storm resembles a supercell and appears to become quite steady by the end of 2 h, and it is possible that larger VMAX0 values might occur if the simulation were extended to longer durations.

c. *Implications for precipitation*

If ambient CAPE increases, one would generally expect an increase in storm updraft intensity, water vapor flux, condensation, and thus precipitation rates at the surface. As shown in the upper half of Table 6, this is true in a broad sense across the entire simulation set, when the (140) persistent and (85) nonpersistent storms are considered together as a single group. Production of both hail and liquid water aloft, and the amounts that reach the ground, increase as CAPE is increased. However, the full 225-experiment simulation set should probably not be used for analysis of trends in precipitation variables because that set includes storms that fail to persist for an entire 2-h simulation. This would bias any analysis toward the environments with nonpersistent storms. When the analysis is confined only to the persistent storms (lower half of Table 6), *environmental CAPE exhibits no significant linear correlation with RMAX or RMAX0.* That is, *the maximum local liquid precipitation rates associated with persistent storms, either aloft or at the ground, bear no significant linear correlation with the ambient CAPE.* In 25 trios of experiments where only CAPE is changed from 800 to 3200 J kg^{-1}, 8 show a steady decrease in RMAX0 as

TABLE 6. Variations in storm precipitation production as CAPE (J kg^{-1}) is increased. Values are given in g kg^{-1}, except for PCPAREA, which is in km^2. For N = 225, each value is the mean of the 60–120-min average of all storms at that CAPE value; for N = 140, averages include only the persistent storms. The total mass of rainwater produced during the simulations (10^{10} kg) is given as TMASS.

(N = 225)	N	HMAX	HMAX0	RMAX	RMAX0	PCPAREA	TMASS
CAPE = 450	9	0.48	0.00	0.95	0.69	50.5	0.24
CAPE = 800	72	2.06	0.02	3.02	2.10	168.9	0.63
CAPE = 2000	72	6.61	0.06	6.50	4.42	438.9	1.40
CAPE = 3200	72	7.87	0.08	6.53	4.37	503.5	1.42
(N = 140)	N	HMAX	HMAX0	RMAX	RMAX0	PCPAREA	TMASS
CAPE = 450	1	2.93	0.01	3.68	2.85	147.5	0.49
CAPE = 800	25	5.54	0.05	7.24	5.07	332.0	1.06
CAPE = 2000	55	8.37	0.08	7.75	5.37	527.2	1.64
CAPE = 3200	59	9.09	0.10	7.24	4.92	580.0	1.61

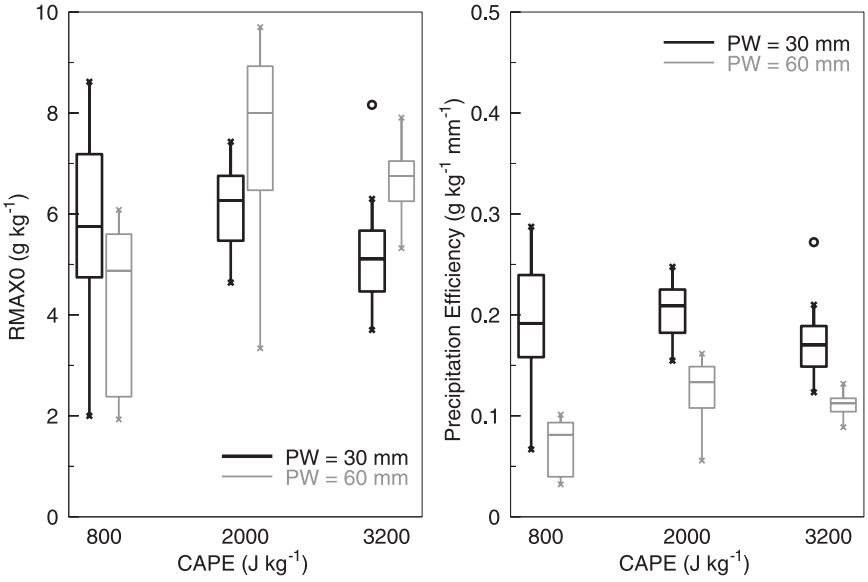

FIG. 11. Box plots (as in Fig. 8) of persistent storm RMAX0, averaged over each experiment's second hour, for 25 sets of 3 experiments with only CAPE varied from 800 to 3200 J kg^{-1}: (left) RMAX0 and (right) PE. Experiments are further binned by PW. Only 1 persistent storm occurred in 9 simulations produced at CAPE = 450 and it is excluded from the figure.

CAPE increases, 5 show a steady increase, and 12 show a peak in RMAX0 at CAPE = 2000. These 25 sets, 75 experiments in all, are binned by CAPE and PW in Fig. 11. Instead of RMAX and RMAX0, it is hail mixing ratios aloft (HMAX) and at the surface (HMAX0) that are strongly tied to CAPE. Of course, HMAX0 is also strongly modulated by PW (which is related to environmental temperature and T_{LCL}): almost no hail reaches the surface in any of the storms in the PW = 60-mm experiments, because of the increased height of the melting level (5 km) compared to the experiments with PW = 30 mm (3 km).

Although the peak local liquid precipitation rates in the persistent storms are not strongly influenced by CAPE, simulations with higher CAPE do produce an increase in the total mass of rainwater that falls to the ground during the simulation (TMASS), as well as the ground area that receives at least 10 mm of liquid precipitation (PCPAREA; Table 6). PCPAREA increases by almost 60% when CAPE is changed from 800 to 2000 J kg^{-1}, all other environmental parameters held equal, with at least a further 10% increase in area occurring when CAPE is raised from 2000 to 3200 J kg^{-1}. This steady increase is attributable to an increase in the number of discrete updrafts of at least 10 m s^{-1} at 2 km AGL identified in the simulations, counted at the last model time step (Fig. 12). There is also some tendency for the instantaneous size of the liquid precipitation footprint (RAREA0, defined as the ground area that received rainfall in the preceding 5 min) to increase as CAPE increases, at least for one set of four simulations with only CAPE changed (Fig. 13). However, this increase is not statistically significant for the transition from CAPE = 2000 to CAPE = 3200. Although individual storm rainfall rates are relatively unchanged

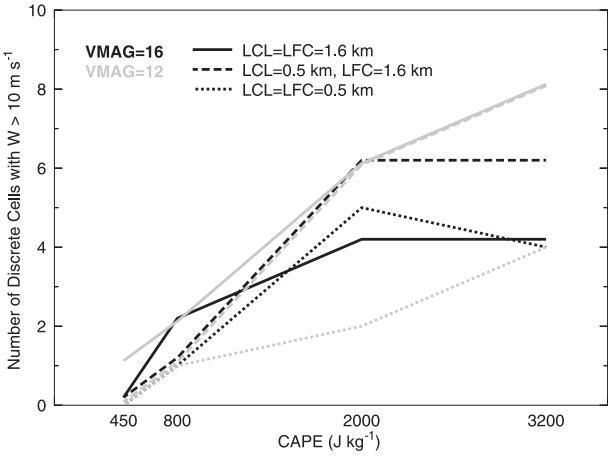

FIG. 12. Number of discrete updrafts of at least 10 m s^{-1} in a subset of the COMPASS simulations, counted at the last model time step (120 min) and at 2 km AGL. Gray lines denote VMAG = 12, and the black lines VMAG = 16. Line styles denote the three possible combinations of LCL and LFC, and each line connects simulations with every other environmental parameter held constant except for CAPE. Traces are slightly offset from their integer values for readability.

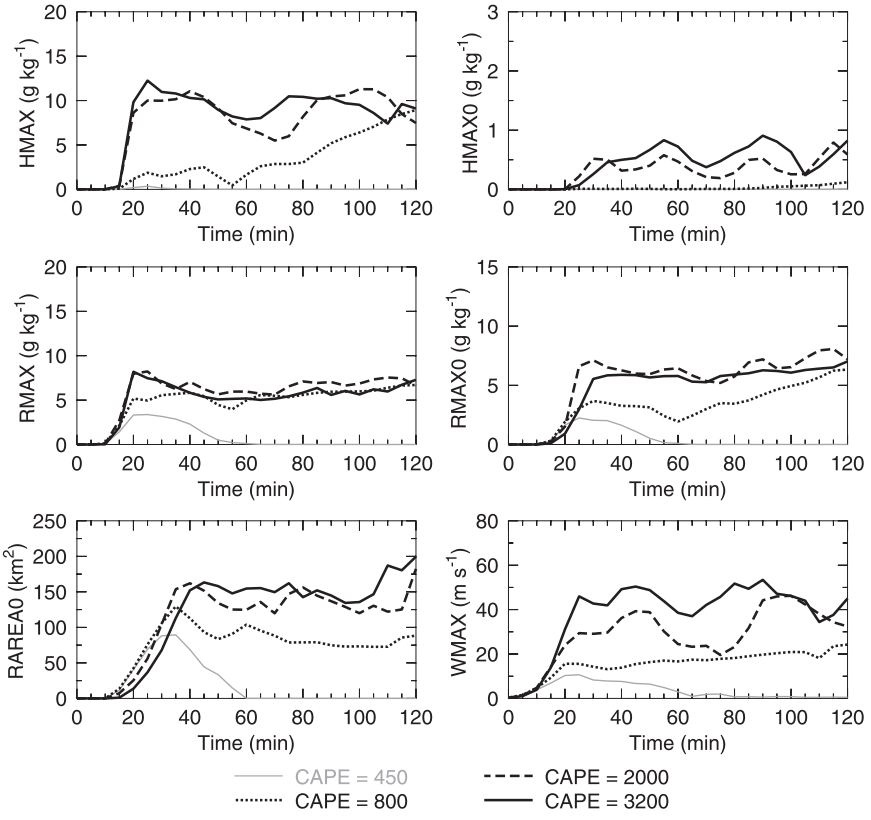

FIG. 13. Time series plots of storm properties from four simulations with only CAPE changed. All simulations shown have VMAG = 16 m s^{-1}, the low value of ZMAXB and ZMAXV, LCL = LFC = 0.5 km, and PW = 30 mm. Acronyms are defined in the text.

when CAPE is at least 800 J kg^{-1}, the marginal increase in storm precipitation footprint and increase in the number of discrete updrafts in each domain likely explain the positive relationship observed between PCPAREA and CAPE. PCPAREA, which is calculated in a ground-relative sense and over an entire 2-h simulation, is also sensitive to the choice of hodograph translation. Thus these PCPAREA results should be viewed as only one example of the rainfall distributions that might occur in the real atmosphere.

Not all of the water vapor that enters a cloud falls out as precipitation. The precipitation efficiency (PE) of a storm may be defined in a number of ways (as described in Sui et al. 2007), most commonly as the ratio of rainfall at the ground to condensation (Ferrier et al. 1996), to water vapor convergence and surface evaporation rates (e.g., Auer and Marwitz 1968; Heymsfield and Schotz 1985; Doswell et al. 1996), or to the precipitable water (Market et al. 2003). In all cases, however, precipitation fallout and PE are directly proportional; that is, storms with greater PE produce more rainfall at the ground, all else held equal. Unfortunately, prior observational studies have struggled with identifying whether a relationship between PE and CAPE exists in the real atmosphere. Marwitz (1972) and Fankhauser (1988) found no clear relationships between CAPE and PE of isolated storms. Statistically insignificant linear correlations between CAPE and PE have also been found in studies of warm-season mesoscale convective systems (Market et al. 2003) and squall lines (Takemi 2007).

Market et al. (2003) has suggested that a curvilinear relationship between CAPE and PE is plausible. In such a relationship, the two are positively correlated up to some unknown ''optimal'' value, and then become negatively correlated, with PE decreasing as CAPE continues to increase. Market et al. (2003, p. 1282) hypothesized that this decrease occurs because ''the strong updraft(s) afforded by a large CAPE would eject too much condensate out of the anvil.''[4] The persistent CAPE = 2000 storms herein do produce substantially more anvil ice (a 200%–300% increase in pristine

[4] The CAPE–PE relationship hypothesized by Market et al. (2003) may also reflect that some CAPE environments (beyond the ''optimal'' CAPE value) are characterized by deep elevated mixed layers, and, presumably, drier air aloft (Lanicci and Warner 1991).

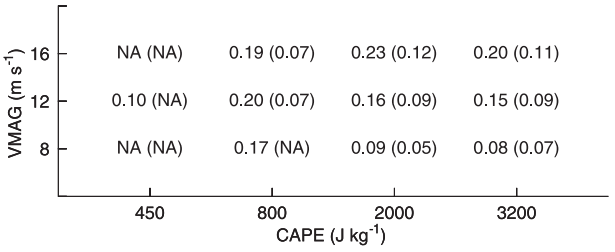

FIG. 14. As in Fig. 5, but for mean second-hour PE, defined in the text as RMAX0 divided by PW. For reference, the highest value of PE (in the given units) at any 5-min output time in any of the 225 simulations is 0.33.

crystals in the 10–16 km AGL layer when compared to the CAPE = 800 storms, and a further 100% increase from CAPE = 2000 to CAPE = 3200), but this fact alone does not guarantee that such a relationship between CAPE and PE exists.

It is straightforward to use the Market et al. (2003) definition of PE to assess our simulations (simply by calculating RMAX0 divided by PW; Fig. 11). McCaul et al. (2005, their Fig. 8) demonstrated that for a set of 12 simulations with CAPE varied from 800 to 3200 J kg^{-1}, the PW = 30 storms featured higher PE compared to those in the PW = 60 environments. Figure 11 shows that this is the case across all simulations explored at CAPE = 800 and greater. Also, the difference in PE between the PW = 30 and PW = 60 groups decreases as CAPE is raised. This is likely because an increase in CAPE allows updrafts to overcome the excessive water loading that occurs at PW = 60. At CAPE = 800, updrafts in environments with the high value of PW are weaker as a result of this water loading, and thus not only produce the smallest amounts of rainfall at the surface but are also the most inefficient rainfall producers in the dataset. However, as with RMAX0, Fig. 11 shows that there is no clear linear trend in PE as the ambient CAPE is changed. The existence of Market et al.'s purported optimal CAPE value finds only modest support in the COMPASS database. Although RMAX0 is clearly greatest for storms in simulations where CAPE = 2000 and PW = 60, a similar maximum in PE is not as obvious.

The impacts of vertical wind shear (in our case, VMAG) on PE are also worthy of discussion. Marwitz (1972) hypothesized that increasing wind shear acts to decrease a storm's PE by increasing entrainment of dry air, causing greater evaporation of potential precipitation. On the contrary, Fankhauser (1988, his Fig. 9) showed essentially no trend in PE as cloud-layer wind shear was increased. In our simulations, average PE increases steadily as VMAG is increased for CAPE = 2000 and CAPE = 3200, but not for CAPE = 800 (Fig. 14). As VMAG is increased at CAPE = 2000 or 3200, updrafts are stronger (Fig. 5 and Table 3), wider (Kirkpatrick et al. 2007, his Fig. 8), and exhibit increased updraft overturning efficiency (the ratio of actual peak updraft speed to the value predicted by parcel theory; McCaul and Cohen 2002), all of which imply more efficient production of precipitation. In our simulations, increased VMAG causes PE to increase, at least when CAPE is 2000 J kg^{-1} or greater (Fig. 14). It would have been impossible for Fankhauser (1988) to diagnose this relationship at similar values of CAPE, as only 2 of the 7 cases in his study involved storms in environments with CAPE above 1800 J kg^{-1}.

4. Summary

The sensitivity of simulated convective storms to storm environment is both directly and indirectly a function of the ambient CAPE. When CAPE is reduced from our moderate or high values (2000 or 3200) to 800 J kg^{-1}, the existence of strong, persistent updrafts becomes a strong function of the vertical distribution of buoyancy. At CAPE = 800, 23 of 36 (64%) simulations with a low vertical level of maximum buoyancy (ZMAXB) produce an updraft that can be tracked for the entirety of a 2-h simulation with a second-hour mean updraft velocity of 10 m s^{-1} or more; when ZMAXB is at our high value, only 2 of 36 (6%) simulations meet these criteria of persistence and strength. When CAPE is reduced further to 450 J kg^{-1}, only 1 out of 9 storms is persistent. The behavior at the 450 and 800 J kg^{-1} CAPE values is in stark contrast to the two higher CAPE values considered here, where more than three-fourths of storms are persistent (76% at CAPE = 2000 and 82% at CAPE = 3200). Both LFC and T_{LCL} have statistically significant correlations to WMAX at all values of CAPE $\geq$ 800 J kg^{-1}.

Two additional aspects of storm morphology, vertical vorticity and precipitation, were also studied in this paper. In simulations where CAPE is 2000 or 3200 J kg^{-1}, correlations between low-level vorticity (VMAX0) and other background environmental parameters (shear, the vertical distribution of buoyancy, and LCL and LFC height) resemble relationships seen in previous climatological studies of strong convection. One of the more interesting results is that a high LFC (1.6 km in this study) correlates with greater vertical vorticity at mid-levels (VMAX), but a low LFC (0.5 km) correlates with greater VMAX0.

At CAPE = 800, however, correlations between environmental parameters and VMAX behave almost identically to those with VMAX0, and are very different from those seen at the higher values of CAPE. In the CAPE = 800 regime, ZMAXB, ZMAXV, and T_{LCL} are

the three parameters that show the strongest correlations to vorticity. When CAPE is reduced further to 450 J kg^{-1}, however, only 1 out of 9 simulations produces a storm with a sizable vertical vorticity in the simulation's second hour (similar to the behavior of updraft velocity), and that storm's peak VMAX0 is lower than 23 of the 25 persistent storms at CAPE = 800. As CAPE decreases below 800 J kg^{-1}, it is increasingly difficult for the simulations to produce not only persistent, strong updrafts, but also strong rotation.

No obvious linear relationship between CAPE and surface rainfall rates is found in the present database in the PW = 30-mm simulations. For simulations with PW = 60 mm, however, there is some evidence that surface rainfall rates are maximized when CAPE is 2000 J kg^{-1}, with lower rates as CAPE is either increased or decreased. Although there is no ''one size fits all'' relationship between CAPE and surface precipitation *rates*, updrafts are slightly larger in diameter and are also more numerous in simulations where CAPE is higher. As a result, there is a positive correlation between increased CAPE and increased total precipitation *over the simulation domain*.

As discussed in Kirkpatrick et al. (2007) and Kirkpatrick et al. (2009), results from this simulation archive are not intended to serve directly as forecast tools or to assert guaranteed relationships between environmental conditions and ''real world'' observed storm properties. No idealized study of simulated storm behavior can claim direct applicability to storms in the real atmosphere. Elmore et al. (2002b) presented simulations in which ''indistinguishably small'' changes to the initial sounding led to ''disproportionately large'' differences in storm longevity, calling into question the use of cloud-scale models as explicit forecasting tools. Even the real-world application of model-derived forecasts of environmental parameters (e.g., CAPE, BRN, or SRH) is fraught with difficulty (Elmore et al. 2002a), and uncertainty bars for these model-derived forecast parameters are frequently quite large (e.g., Thompson et al. 2003, 2007). The use and utility of diagnostic variables derived from the sounding in forecasting convective storm evolution is also open to question (Doswell and Schultz 2006), and each of the sounding parameters discussed herein should be similarly scrutinized.

Instead, these analyses serve mainly to isolate and clarify key aspects of the environmental sounding that influence storm morphology and evolution, and to help quantify or rank the strength of those relationships and their trends within the parameter space. We believe that these results can best be used to motivate additional study of convective storm behavior, in both the numerical and observational realms, and to serve as a starting framework for those studies. For regimes where CAPE is below roughly 1000 J kg^{-1}, the sensitivity of real storms to other environmental factors discussed here has not been adequately studied with sufficiently careful control. Additional analysis of existing datasets of observed storms in these CAPE regimes (such as in Johns et al. 1993; Davies 2006b) could be revealing, given the number of severe weather events that occur under such conditions. A larger set of numerical simulations with CAPE values below 800 J kg^{-1}, and also between the values of 800 and 2000 J kg^{-1} which were explored here, may also be beneficial to more clearly diagnosing the influences of ZMAXB and PW, as well as to provide additional insight into the possibility of a CAPE–shear or other environmental parameter combination that might promote a maximum in updraft overturning or precipitation efficiency.

The effects of environmental humidity (FTRH) on deep convection must also be considered, as James and Markowski (2010) observed that simulated convective storms at an extreme value of CAPE (4500 J kg^{-1}) are not influenced much by environmental dry air, but the effects are much greater at lower CAPE values. Preliminary analysis of the COMPASS results indicates that the survivability of updrafts in environments having FTRH less than 90% appears to depend upon LCL and LFC heights, implying the importance of the not-unexpected role of entrainment on smaller-diameter updrafts. There is also a need to perform sensitivity studies of the impact of model mixing and turbulence schemes before drawing final conclusions. While the COMPASS simulation framework provides a foundation for studying the important effects of reduced FTRH on convective storms, pursuit of such research lies beyond the scope of the present paper, and must be deferred to the future.

Acknowledgments. This research was supported by a grant from the National Oceanic and Atmospheric Administration (NOAA) to Dr. Kevin Knupp at UA Huntsville (Grant NA08OAR4600896). Publication support was provided by the Earth System Science Center at UA Huntsville. We appreciate the detailed reviews provided by Dr. David Schultz (Chief Editor), Stephen Corfidi, and three additional anonymous reviewers; their constructive criticisms have resulted in a greatly improved manuscript. We acknowledge computing support from Scott Podgorny (UAH) and Jayanthi Srikishen of USRA in Huntsville. Original support for the COMPASS simulations was provided in 2002 through Grant ATM-0126408 from the National Science Foundation, under the supervision of Dr. Stephan Nelson. (For additional information, please see the COMPASS Web site at http://space.hsv.usra.edu/COMPASS/.)

REFERENCES

Adlerman, E. J., and K. K. Droegemeier, 2005: The dependence of numerically simulated cyclic mesocyclogenesis upon environmental vertical wind shear. *Mon. Wea. Rev.,* **133,** 3595–3623.

Auer, A. H., Jr., and J. D. Marwitz, 1968: Estimates of air and moisture flux into hailstorms on the High Plains. *J. Appl. Meteor.,* **7,** 196–198.

Brooks, H. E., 2009: Proximity soundings for severe convection for Europe and the United States from reanalysis data. *Atmos. Res.,* **93,** 546–553.

——, A. R. Anderson, K. Riemann, I. Ebbers, and H. Flachs, 2007: Climatological aspects of convective parameters from the NCAR/NCEP reanalysis. *Atmos. Res.,* **83,** 294–305.

Browning, K. A., 1962: Cellular structure of convective storms. *Meteor. Mag.,* **91,** 341–350.

——, 1964: Airflow and precipitation trajectories within severe local storms which travel to the right of the winds. *J. Atmos. Sci.,* **21,** 634–639.

Bryan, G. H., J. C. Wyngaard, and J. M. Fritsch, 2003: Resolution requirements for the simulation of deep moist convection. *Mon. Wea. Rev.,* **131,** 2394–2416.

Bunkers, M. J., B. A. Klimowski, J. W. Zeitler, R. L. Thompson, and M. L. Weisman, 2000: Predicting supercell motion using a new hodograph technique. *Wea. Forecasting,* **15,** 61–79.

——, J. S. Johnson, L. J. Czepyha, J. M. Grzywacz, B. A. Klimowski, and M. R. Hjelmfelt, 2006: An observational examination of long-lived supercells. Part II: Environmental conditions and forecasting. *Wea. Forecasting,* **21,** 689–714.

Chin, H.-N. S., and R. B. Wilhelmson, 1998: Evolution and structure of tropical squall-line environments within a moderate CAPE and strong low-level jet environment. *J. Atmos. Sci.,* **55,** 3089–3113.

Cohen, C., and E. W. McCaul Jr., 2006: The sensitivity of simulated convective storms to variations in prescribed single-moment microphysics parameters that describe particle distributions, sizes, and numbers. *Mon. Wea. Rev.,* **134,** 2547–2565.

——, and ——, 2007: Further results on the sensitivity of simulated storm precipitation efficiency to environmental temperature. *Mon. Wea. Rev.,* **135,** 1671–1684.

Colman, B. R., 1990: Thunderstorms above frontal surfaces without positive CAPE. Part I: A climatology. *Mon. Wea. Rev.,* **118,** 1103–1122.

Cotton, W. R., and R. A. Anthes, 1989: *Storm and Cloud Dynamics*. Academic Press, 881 pp.

Craven, J. P., and H. E. Brooks, 2004: Baseline climatology of sounding derived parameters associated with deep, moist convection. *Natl. Wea. Dig.,* **28,** 13–24.

Davies, J. M., 2004: Estimations of CIN and LFC associated with tornadic and nontornadic supercells. *Wea. Forecasting,* **19,** 714–726.

——, 2006a: Hurricane and tropical cyclone tornado environments from RUC proximity soundings. Preprints, *23rd Conf. on Severe Local Storms,* St. Louis, MO, Amer. Meteor. Soc., 12.6A. [Available online at http://ams.confex.com/ams/23SLS/techprogram/paper_115483.htm.]

——, 2006b: RUC soundings with cool season tornadoes in ''small'' CAPE settings and the 6 November 2005 Evansville, Indiana tornado. Preprints, *23rd Conf. on Severe Local Storms,* St. Louis, MO, Amer. Meteor. Soc., 4.3. [Available online at http://ams.confex.com/ams/23SLS/techprogram/paper_115477.htm.]

Dean, A. R., R. S. Schneider, R. L. Thompson, J. Hart, and P. D. Bothwell, 2009: The conditional risk of severe convection estimated from archived NWS/Storm Prediction Center mesoscale objective analyses: Potential uses in support of forecast operations and verification. Preprints, *23rd Conf. on Weather Analysis and Forecasting/19th Conf. on Numerical Weather Prediction,* Omaha, NE, Amer. Meteor. Soc., 6A.5. [Available online at http://ams.confex.com/ams/23WAF19NWP/techprogram/paper_154304.htm.]

Doswell, C. A., III, and D. M. Schultz, 2006: On the use of indices and parameters in forecasting severe storms. *Electron. J. Severe Storms Meteor.,* **1** (3), 1–22.

——, H. E. Brooks, and R. A. Maddox, 1996: Flash flood forecasting: An ingredients-based methodology. *Wea. Forecasting,* **11,** 560–581.

Droegemeier, K. K., S. M. Lazarus, and R. P. Davies-Jones, 1993: The influence of helicity on numerically simulated convective storms. *Mon. Wea. Rev.,* **121,** 2005–2029.

Elmore, K. L., D. J. Stensrud, and K. C. Crawford, 2002a: Ensemble cloud model applications to forecasting thunderstorms. *J. Appl. Meteor.,* **41,** 363–383.

——, ——, and ——, 2002b: Explicit cloud-scale models for operational forecasts: A note of caution. *Wea. Forecasting,* **17,** 873–884.

Esterheld, J. M., and D. J. Giuliano, 2008: Discriminating between tornadic and non-tornadic supercells: A new hodograph technique. *Electron. J. Severe Storms Meteor.,* **3** (2), 1–50.

Evans, J. S., and C. A., Doswell III, 2001: Examination of derecho environments using proximity soundings. *Wea. Forecasting,* **16,** 329–342.

Fankhauser, J. C., 1988: Estimates of thunderstorm precipitation efficiency from field measurements in CCOPE. *Mon. Wea. Rev.,* **116,** 663–684.

Ferrier, B. S., J. Simpson, and W.-K. Tao, 1996: Factors responsible for precipitation efficiencies in midlatitude and tropical squall-line simulations. *Mon. Wea. Rev.,* **124,** 2100–2125.

Geerts, B., T. Andretta, S. J. Luberda, J. Vogt, Y. Wang, L. D. Oolman, J. Finch, and D. Bikos, 2009: A case study of a long-lived tornadic mesocyclone in a low-CAPE complex-terrain environment. *Electron. J. Severe Storms Meteor.,* **4** (3), 1–29.

Heymsfield, G. M., and S. Schotz, 1985: Structure and evolution of a severe squall line over Oklahoma. *Mon. Wea. Rev.,* **113,** 1563–1589.

Horgan, K. L., D. M. Schultz, R. H. Johns, J. E. Hales, and S. F. Corfidi, 2007: A five-year climatology of elevated severe convective storms in the United States east of the Rocky Mountains. *Wea. Forecasting,* **22,** 1031–1044.

James, R. P., and P. M. Markowski, 2010: A numerical investigation of the effects of dry air aloft on deep convection. *Mon. Wea. Rev.,* **138,** 140–161.

Johns, R. H., J. M. Davies, and P. W. Leftwich, 1993: Some wind and instability parameters associated with strong and violent tornadoes. 2. Variations in the combinations of wind and instability parameters. *The Tornado: Its Structure, Dynamics, Hazards, and Prediction, Geophys. Monogr.,* Vol. 79, Amer. Geophys. Union, 583–590.

Kennedy, P. C., N. E. Westcott, and R. W. Scott, 1993: Single-Doppler radar observations of a mini-supercell tornadic thunderstorm. *Mon. Wea. Rev.,* **121,** 1860–1870.

Kerr, B. W., and G. L. Darkow, 1996: Storm-relative winds and helicity in the tornadic thunderstorm environment. *Wea. Forecasting,* **11,** 489–505.

Kirkpatrick, C., E. W. McCaul Jr., and C. Cohen, 2007: The motion of simulated convective storms as a function of basic environmental parameters. *Mon. Wea. Rev.,* **135,** 3033–3051.

——, ——, and ——, 2009: Variability of updraft and downdraft characteristics in a large parameter space study of convective storms. *Mon. Wea. Rev.,* **137,** 1550–1561.

Klemp, J. B., and R. B. Wilhelmson, 1978: The simulation of three-dimensional convective storm dynamics. *J. Atmos. Sci.,* **35,** 1070–1096.

Knupp, K. R., J. R. Stalker, and E. W. McCaul, 1998: An observational and numerical study of a mini-supercell storm. *Atmos. Res.,* **49,** 35–63.

Lanicci, J. M., and T. T. Warner, 1991: A synoptic climatology of the elevated-mixed layer inversion over the southern Great Plains in spring. Part I: Structure, dynamics, and seasonal evolution. *Wea. Forecasting,* **6,** 181–197.

Maddox, R. A., 1976: An evaluation of tornado proximity wind and stability data. *Mon. Wea. Rev.,* **104,** 133–142.

Market, P., S. Allen, R. Scofield, R. Kuligowski, and A. Gruber, 2003: Precipitation efficiency of warm-season Midwestern mesoscale convective systems. *Wea. Forecasting,* **18,** 1273–1285.

Markowski, P. M., and J. M. Straka, 2000: Some observations of rotating updrafts in a low-buoyancy, highly sheared environment. *Mon. Wea. Rev.,* **128,** 449–461.

——, C. Hannon, J. Frame, E. Lancaster, A. Pietrycha, R. Edwards, and R. L. Thompson, 2003: Characteristics of vertical wind profiles near supercells obtained from the Rapid Update Cycle. *Wea. Forecasting,* **18,** 1262–1272.

Marwitz, J. D., 1972: Precipitation efficiency of thunderstorms on the High Plains. *J. Res. Atmos.,* **6,** 367–370.

McCaul, E. W., Jr., 1991: Buoyancy and shear characteristics of hurricane–tornado environments. *Mon. Wea. Rev.,* **119,** 1954–1978.

——, and M. L. Weisman, 1996: Simulations of shallow supercell storms in landfalling hurricane environments. *Mon. Wea. Rev.,* **124,** 408–429.

——, and ——, 2001: The sensitivity of simulated supercell structure and intensity to variations in the shapes of environmental buoyancy and shear profiles. *Mon. Wea. Rev.,* **129,** 664–687.

——, and C. Cohen, 2002: The impact on simulated storm structure and intensity of variations in the mixed layer and moist layer depths. *Mon. Wea. Rev.,* **130,** 1722–1748.

——, ——, and C. Kirkpatrick, 2005: The sensitivity of simulated storm structure, intensity, and precipitation efficiency to environmental temperature. *Mon. Wea. Rev.,* **133,** 3015–3037.

Miglietta, M. M., and R. Rotunno, 2010: Numerical simulations of low-CAPE flows over a mountain ridge. *J. Atmos. Sci.,* **67,** 2391–2401.

Monteverdi, J. P., and J. Quadros, 1994: Convective and rotational parameters associated with three tornado episodes in Northern and Central California. *Wea. Forecasting,* **9,** 285–300.

Montgomery, D. C., and G. C. Runger, 2003: *Applied Statistics and Probability for Engineers*. 3rd ed. Wiley and Sons, Inc., 706 pp.

Moore, J. T., A. C. Czarnetzki, and P. S. Market, 1998: Heavy precipitation associated with elevated thunderstorms formed in a convectively unstable layer aloft. *Meteor. Appl.,* **5,** 373–384.

Rasmussen, E. N., 2003: Refined supercell and tornado forecast parameters. *Wea. Forecasting,* **18,** 530–535.

——, and D. O. Blanchard, 1998: A baseline climatology of sounding-derived supercell and tornado forecast parameters. *Wea. Forecasting,* **13,** 1148–1164.

——, and J. M. Straka, 1998: Variations in supercell morphology. Part I: Observations of the role of upper-level storm-relative flow. *Mon. Wea. Rev.,* **126,** 2406–2421.

Rotunno, R., and J. B. Klemp, 1982: The influence of the shear-induced pressure-gradient on thunderstorm motion. *Mon. Wea. Rev.,* **110,** 136–151.

Sui, C.-H., X. Li, and M.-J. Yang, 2007: On the definition of precipitation efficiency. *J. Atmos. Sci.,* **64,** 4506–4513.

Takemi, T., 2007: Environmental stability control of the intensity of squall lines under low-level shear conditions. *J. Geophys. Res.,* **112,** D24110, doi:10.1029/2007JD008793.

Thompson, R. L., and R. Edwards, 2000: An overview of environmental conditions and forecast implications of the 3 May 1999 tornado outbreak. *Wea. Forecasting,* **15,** 682–699.

——, ——, J. A. Hart, K. L. Elmore, and P. Markowski, 2003: Close proximity soundings within supercell environments obtained from the Rapid Update Cycle. *Wea. Forecasting,* **18,** 1243–1261.

——, C. M. Mead, and R. Edwards, 2007: Effective storm-relative helicity and bulk shear in supercell thunderstorm environments. *Wea. Forecasting,* **22,** 102–115.

Trapp, R. J., D. M. Schultz, A. V. Ryzhkov, and R. L. Holle, 2001: Multiscale structure and evolution of an Oklahoma winter precipitation event. *Mon. Wea. Rev.,* **129,** 486–501.

van den Broeke, M. S., D. M. Schultz, R. H. Johns, J. S. Evans, and J. E. Hales, 2005: Cloud-to-ground lightning producting in strongly forced, low-instability convective lines associated with damaging wind. *Wea. Forecasting,* **20,** 517–530.

van den Heever, S. C., and W. R. Cotton, 2004: The impact of hail size on simulated supercell storms. *J. Atmos. Sci.,* **61,** 1596–1609.

Weisman, M. L., 1993: The genesis of severe, long-lived bow echoes. *J. Atmos. Sci.,* **50,** 645–670.

——, and J. B. Klemp, 1982: The dependence of numerically simulated convective storms on vertical wind shear and buoyancy. *Mon. Wea. Rev.,* **110,** 504–520.